RBF and SVM Neural Networks for Automated Power Quality Events Classification

Przemysław Janik, Tadeusz Łobos

Wroclaw University of Technology, ul. Wyb. Wyspiańskiego 27, 50-370 Wroclaw, Poland,
tel. +48713202901, fax +48713202006,
e-mail:przemyslaw.janik@pwr.wroc.pl, tadeusz.lobos@pwr.wroc.pl

Abstract- This paper presents classification results of different power quality disturbances. SVM and RBF neural networks are considered as appropriate classifiers for power quality issues, however SVM networks show better performance. Simulation of disturbed signals by parametric equations enabled the assessment of signal parameters influence on classification rate. Positive results encouraged further research. Model of supply system suffering from sags was simulated. Independent from line length and sag duration the classifier was set to recognize different sag types. The idea of space phasor was applied to obtain distinctive patterns from three phase system. Wavelet transform was used to find the beginning of sags. Positive classification results were obtained**.**

I. Introduction

The power quality issues raise recently vivid attention by the industry and scientific community [1], [2]. Different reasons can be named [3].
The deregulation of the electricity marked has caused growing need for standardization and performance criteria [4]. Electricity customers have become more aware of their rights for low-cost electricity of high reliability and quality.
Generation of electrical energy take place in large power stations connected to the transmission system and smaller units connected at low voltage levels. Wind generators are often connected via power electronic devices. The problems of voltage stability and harmonic generation arise [5].
Electronic and power electronic equipment has become more sensitive to voltage disturbances than its counterparts years ago [2]. Modern power electronic equipment is not only sensitive to voltage disturbances it also causes disturbances for other customers [6].
The ideal voltage curve in a three phase public electrical network should be characterized as follows [4]: pure sinus form, constant frequency according to the grid frequency, equal amplitudes in each phase according to the voltage level, defined phase-sequence with an angle of 120° between them. Every phenomenon which affects those parameters will be seen as decrease in voltage quality.
Some main disturbances types are named in [7]. In the first attempt five typical disturbances were simulated using parametric equations. Positive results encouraged further research.
One of the common disturbances is voltage sag originating in short circuits. Model of supply system was build to determine the classification ability of different sag types for neural networks classifiers. The influence of line length, sag duration, and resistance was evaluated, totally 2800 cases.

II. Support Vector Machines

In recent years, a new approach was developed to construct and train neural networks, which is free of such disadvantages [8], as local minima or complexness of the architecture. New networks are called Support Vector Machines (SVM) [8, 9].
SVM implements a special training algorithm maximizing the separating margin between two classes, given by a set of data pairs (sample, class)

$$(x_i, d_i) \tag{1}$$

SVMs are unidirectional, have two layers and can implement different activation functions: linear, polynomial, radial or sigmoidal.
For linear separable training pairs of two classes (1) the separating hyper plane is given by

$$g(x) = w^T x + b = 0 \tag{2}$$

A hyper plane (2) is considered optimal when the separating margin between two classes is maximal and this is achieved by computing

$$\min_{w} \frac{1}{2} w^T w \tag{3}$$

and considering

$$d_i \left(w^T x_i + b \right) \geq 1 \tag{4}$$

This problem means minimizing the Lagrange function

$$J\left(w, b, \alpha\right) = \frac{1}{2} w^T w - \sum_{i=1}^{p} \alpha_i \left[d_i \left(w^T x_i + b \right) - 1 \right] \tag{5}$$

If two classes are not linearly separable the equations (3) and (4) have different forms

$$\phi\left(w, \xi\right) \frac{1}{2} w^T w + C \sum_{i=1}^{p} \xi_i, \quad \xi_i > 0 \tag{6}$$

$$d_i \left(w^T x_i + b \right) \geq 1 - \xi_i \tag{7}$$

where ξ is so called fulfilling variable.

In this case, the SVM maps the input vectors into a high dimensional space through some nonlinear mapping, where an optimal hyper plane is constructed.

Good classification properties of SVM have been obtained [9]. An simplified structure of SVM neural network is shown in Fig. 1.

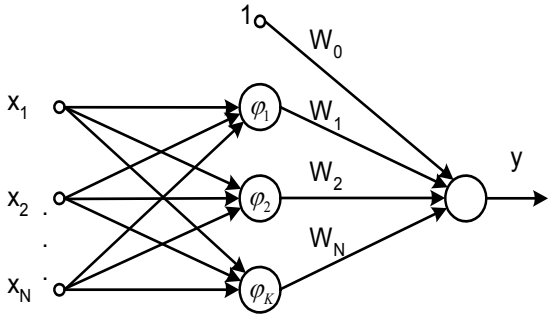

Figure 1. Simplified structure of SVM neural network

II. Radial Basis Function Networks

Radial basis networks [10, 11, 12] consist of two layers: a hidden radial basis layer and an output linear layer (Fig. 2). The hidden-layer neurons have centroids $\mathbf{c}_i$ and smoothing factors (bias) $\mathbf{b}_i$ (i=1,2,…,N , where N is the number of vectors in the hidden-layer). These neurons compute the vector distance between the input vector **p** and the centroid $\mathbf{c}_i$. The neuron outputs are nonlinear, radially symmetric functions of the distance. A commonly used transfer function for a radial basis neuron is the Gaussian exponential function

$$\mathrm{f}(x) = e^{-x^2} \tag{8}$$

Thus, the output of the neuron is strongest when the input vectors **p** are the nearest to the $\mathbf{c}_i$. The bias $\mathbf{b}_i$ allows the sensitivity of the radial basis neuron to be adjusted.

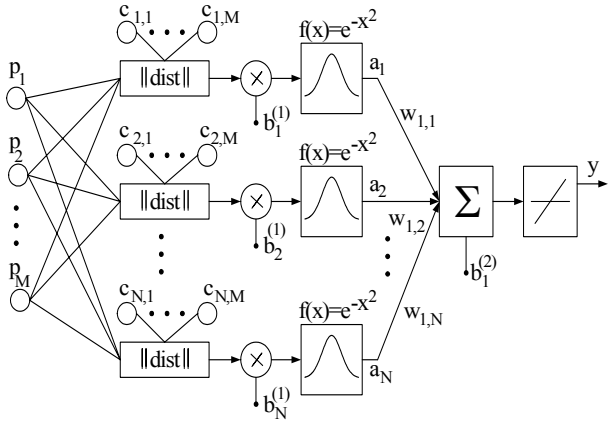

Figure 2. Architecture of radial basis function neural network

The network is initialized by setting the centroids $\mathbf{c}_i$ equal to the training patterns (training input vectors) $\mathbf{p}^{(T)}$.
If an input vector is presented to such a network, each neuron in the radial basis hidden-layer will have at the output a value according to how close the input vector is to one of the input training vectors. The output weight $\mathbf{w}_i$ pass the output value to the linear neuron in second layer.

III. Space Phasor

In order to construct sufficiently distinctive patterns for the SVM classifier, the idea of the space phasor was applied [13]. Construction of a space phasor requires three-phase signal. Complex space vector **f** is given by (9)

$$\begin{bmatrix} f_1 \\ f_2 \end{bmatrix} = \sqrt{\frac{2}{3}} \begin{bmatrix} 1 & -\frac{1}{2} & -\frac{1}{2} \\ 0 & \frac{\sqrt{3}}{2} & -\frac{\sqrt{3}}{2} \end{bmatrix} \begin{bmatrix} f_a \\ f_b \\ f_c \end{bmatrix} \tag{9}$$

and

$$\mathbf{f} = \frac{f_1 + jf_2}{\sqrt{2}} \tag{10}$$

A further step in transforming the input data for the classifier and obtaining slightly different patterns can be undertaken. It means stopping the spinning space vector by multiplication with the operator $e^{j\omega t}$, where is the angular velocity of the fundamental component.

IV. Classification of Signals Given by Equations

A. Signal Simulation

Signal modelling by parametric equations for classifier tests makes it possible to change the curve shape (signal parameters) in wide range and controlled manner. Signals belonging to six main groups were simulated, which are typical for one and three phase systems. Signal without disturbances, pure sinusoid, was a special reference class. Equations representing signals in each class are summarized in Tab. 1.

Table 1. Parametric equation and parameters change range for simulation of disturbed signals

Event	Equation	Parameters change range
pure sinusoid	$v(t) = \sin(\omega t)$	amplitude: 1 frequency: 50 Hz
sudden sag	$v(t) = \left(1 - \alpha_{zn}\left(1(t-t_1) - 1(t-t_2)\right)\right)\sin(\omega t)$	duration: $(t_2 - t_1) = 0...9T$ amplitude: $\alpha_{zn} = 0.3...0.8$
sudden swell	$v(t) = \left(1 + \alpha_{pr}\left(1(t-t_1) - 1(t-t_2)\right)\right)\sin(\omega t)$	duration: $(t_2 - t_1) = 0...8T$ amplitude $\alpha_{pr} = 0.3...0.8$
harmonics	$v(t) = \sin(\omega t) + \alpha_{h3}\sin(3\omega t)...$ $+ \alpha_{h5}\sin(5\omega t) + \alpha_{h7}\sin(7\omega t)$	order: 3,5,7 amplitude: $\alpha_h = 0...0.9$
voltage flicker	$v(t) = \left(1 + \alpha_f \sin(\beta_f \omega t)\right)\sin(\omega t)$	frequency: $f_f = 5...10Hz$ amplitude: $\alpha_f = 0.1...0.2$
oscillatory transient	$v(t) = \left(\sin(\omega t) + \alpha_{osc}\exp\left(-(t-t_1)/\tau_{osc}\right)\right)\cdot$ $...\sin\left(\omega_{nosc}(t-t_1)\right)$	time constant: $\tau_{osc} = 0.008...0.04s$ frequency $f_{osc} = 100...400Hz$

One phase signal equations are given but three phase signals were actually simulated. In each phase the signal was identical, only shifted by 120°. The signal amplitude was normalized (1 p.u.) and frequency of main component was set to 50 Hz. The pattern for the classifier was recorded using nine periods' measurement window by sampling frequency of 5 kHz. Every input vector had 900 points. The parameters change ranges are also given in Tab. 1. Only the pure sinusoid, as a reference signal, was unchanged.
Fig. 3 depicts an example of disturbances - oscillatory transients in three phase signal. The time constant was 0.0208 s and oscillations frequency 222 Hz (oscillations period 0.0045 s). Fig. 4 shows

trajectory of rotating space phasor. For an undisturbed signal it would be a circle. The rotating space phasor is used as pattern for the classifiers.

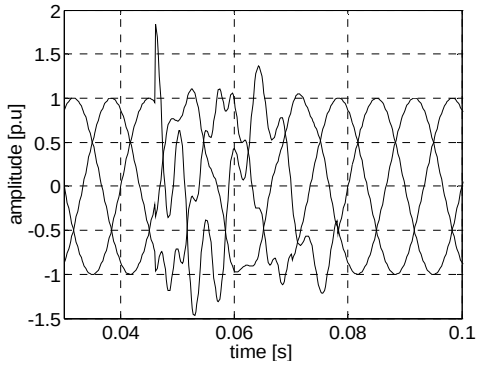

Figure 3. Oscillatory transient in three phase voltage signal

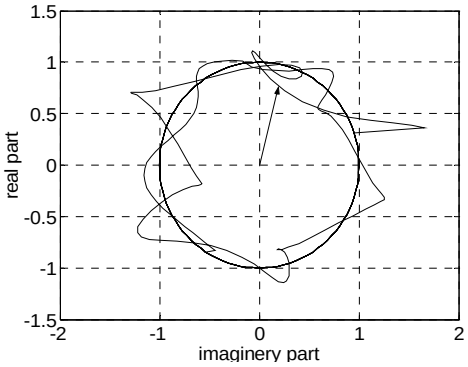

Figure 4. Oscillatory transient, rotating space phasor

Fig. 5 and Fig. 6 are examples of another common disturbance and its representation with rotating space phasor. The amplitude of the depicted voltage flicker was 0.14% of the main component and frequency was 22% of 50 Hz (11 Hz). For this class of disturbances typical are circles with slightly changing radius. They are significantly different from the oscillatory transients' trajectory.

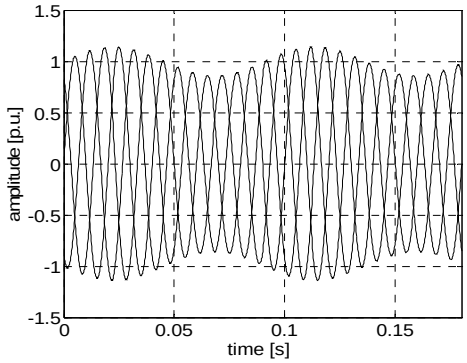

Figure 5. Voltage flicker in a three phase signal

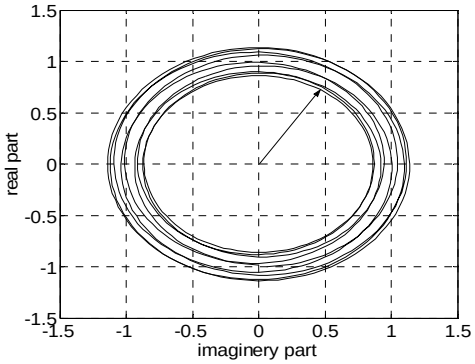

Figure 6. Voltage flicker, rotating space phasor

B. Classification Results

Every class of disturbed signals was represented by 50 different signals. The parameters of the signals covered the range given in the Tab. 1. Ten signal of each class with parameters evenly covering the change range (Tab. 1) were transformed to space phasors and used for training. Remaining vectors were used in the test phase. The classification results are summarized in the Tab. 2, for RBF and SVM classifier respectively. The tables should be interpreted as follows. The column indicates the class. Every row gives the information how many simulated signals were actually correctly recognized (bold) or misinterpreted as other disturbances. The number in every cell is the relation between classified and total number of vectors in each class. SVM classifier shows slightly better performance.

Table 2. Classification results of RBF and SVM classifiers

	Classification rates of RBF network						**Classification rates of SVM network**					
	Sinus	**Swell**	**Flick**	**Hrm**	**Osc**	**Sag**	**Sinus**	**Swell**	**Flick**	**Hrm**	**Osc**	**Sag**
Sinus	**1.0**	0.0	0.0	0.0	0.0	0.0	**1.0**	0.0	0.0	0.0	0.0	0.0
Swell	0.275	**0.725**	0.0	0.0	0.0	0.0	0.025	**0.975**	0.0	0.0	0.0	0.0
Flick	0.0	0.0	**1.0**	0.0	0.0	0.0	0.0	0.0	**1.0**	0.0	0.0	0.0
Hrm	0.025	0.0	0.0	**0.975**	0.0	0.0	0.025	0.0	0.0	**0.975**	0.0	0.0
Osc	0.350	0.0	0.0	0.0	**0.650**	0.0	0.0	0.0	0.0	0.0	**1.0**	0.0
Sag	0.275	0.0	0.0	0.0	0.0	**0.725**	0.025	0.0	0.0	0.0	0.0	**0.975**

VI. Model of Supply System Affected by Voltage Sags – Simulation and Classification Results

A. Supply System Modeling

The study involved a 15 kV supply system modeled in the Matlab environment using Power System Blockset. The diagram of the system is shown in Fig. 2.

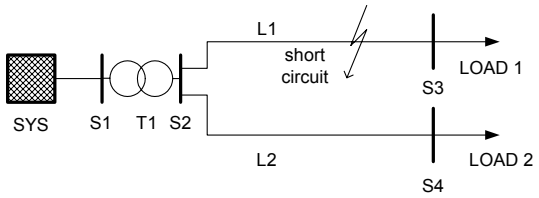

Figure 7. Model of supply system

The System (SYS) describes the initial short circuit apparent power S_k"=3 GVA and voltage level of 110 kV. T1 is a two-winding (delta/star isolated) 110/15kV distribution transformer with S_n=10 MVA. L1 and L2 are typical overhead lines with the lengths 0.5 km and 5 km respectively. Both lines are charged with RL loads LOAD 1 (2 MW) and LOAD 2 (3 MW). S1 to S4 are buses. The short circuit occurs at the end of the line L1. Two fault types were simulated: two-phase and three-phase short circuits. The faults were simulated with a fault block, which allowed switching off a fault not as an ideal breaker, but during the zero crossing time.
Different sag types were simulated: ABC, AB, BC, CA. This sag types were chosen according to faults seen as one of voltage sags origins in supply networks. Signal modeling through parametric equation allowed direct influence on the signal form. In this case it is done indirectly through change of models parameters such as faulted line length. This approach was useful in evaluation of the influence of system parameters change on classification of different voltage sags. Sampling frequency and measurement window length were constant for all research.

B. Simulation and Classification Results

The neural classifier was set to recognize different sag types (ABC, AB, BC, CA) independent from supply system parameters such as faulted line length, short circuit resistance and duration of the sag. Totally 2800 different signals were simulated and analyzed.
The beginning of sags was accurately determined using the wavelet transform [14, 15].

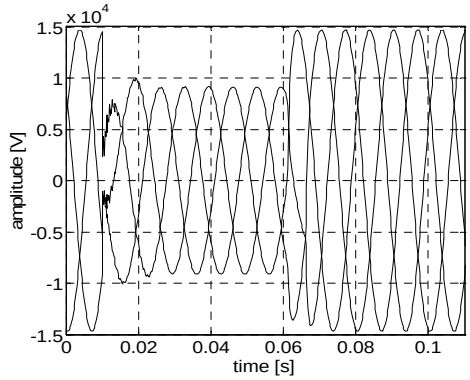

Figure 8. Three phase voltage sag

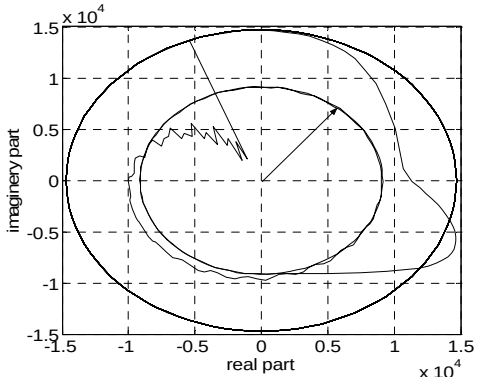

Figure 9. Voltage sag, rotating space vector

Fig. 8 shows an example of a symmetrical three phase voltage sag. Rotating space phasor of this sag shows Fig. 9. Unsymmetrical voltage sags are represented by rotating space phasor in the form of ellipse which position depends on sag type and is significant for the classifier.
Using rotating space phasor as input signal for SVM classifier satisfactory classification results were reached. For short circuit resistance $R_{SC}\approx 0$ only two randomly chosen training vectors were sufficient to recognize others errorless. However the training vectors shouldn't be from one edge of the vectors set. This changed for higher values of R_{SC}. Tab. 3 shows results of ABC sags classification for R_{SC}=5 Ω. To improve the classification the number of training vectors was increased up to 10 and R_{SC} for training vectors was set to 0. The classification mistakes accrued for ABC sags of shortest duration (0.051 to 0.131 s.). Two phase unsymmetrical sags were classified correctly. All other parameters varied in the range equal for all experiments.

Table 3. Classification of ABC sags for R_{sc}=5

L_1 line length	ABC	AB	BC	AC
0.5 km	**0.9**	0.0	0.1	0.0
1.5 km	**0.9**	0.1	0.0	0.0
2.5 km	**0.8**	0.0	0.0	0.2

Tab. 4 shows the most severe case of the research. It marks the limit of classification abilities. 10 used training vectors were obtained for $R_{SC}\approx 0$. The test vectors were obtained for R_{SC}=150 . All other parameters varied in the range given in the Tab. VI. No one symmetrical sag has been classified. Only unsymmetrical sags were recognized.

Table 4. Classification of sags for R_{sc}=150

	ABC	AB	BC	AC
ABC	**0.0**	0.0	0.0	1.0
AB	0.0	**0,8667**	0,1333	0.0
BC	0.0	0.0	**0.9000**	0.1
AC	0.0	0.0	0.0	**1.0**

VII. Conclusion

Power quality disturbances simulated by parametric equations were used to evaluate the classification abilities of RBF and SVM classifiers. After many tests, the SVM networks had shown slightly better classification performance and were used for further research on voltage sag classification.
The space vector representation of a three-phase signal was considered as appropriate input pattern for the classifiers.
Voltage sags originate mainly in faults on another feeder of the network. Four types of voltage sags were simulated. The influences of line length, fault duration and resistance variation on the classification rate were investigated. The wavelet transform turn out to be an adequate method for finding the beginning of an PQ event.
Satisfactory classification rates were achieved with Support Vector Machines during this investigation.

VIII. References

[1] J. Arrilaga, N. R. Watson, S. Chen, *Power System Quality Assessment*, John Wiley&Sons, New York, 2000
[2] M. H. J. Bollen, *What is power quality?*, Electric Power System Research, No. 66, pp. 5-14, 2003
[3] M. H. J. Bollen *Understanding Power Quality Problems Voltage Sags and Interruptions,* IEEE Press, New York, 2000
[4] R. C. Dugan, M. F. McGranaghan, H. W. Beaty, *Electrical Power System Quality*, McGraw-Hill, New York, 1996
[5] M. A. B. Amora, U. H. Bezerra *Assessment of the Effects of Wind Farms Connected in a Power System* in Proc. 2001 IEEE Porto Power Tech Conference, DRS3-260
[6] T. Sakkos, V. Sarv, J. Soojarv, *Efficient Harmonic Distortion Reduction in Diode-Bridge Rectifiers Using Parallel Re-Rectification of theRipple Power,* Electrical Power Quality and Utilization, Conference Proceedings, Cracow Poland, 1999, pp.383-390
[7] J. Mindykowski *Assessment of Electric Power Quality in Ship Systems Fitted with Converter Subsystems*, Gdańsk: Shipbuilding and Shipping, 2003, p.152-164
[8] V. Vapnik, *Statistical Learning Theory*, Wiley, New York, 1998
[9] T. Joachims, Making large-Scale SVM Learning Practical. Advances in Kernel Methods - Support Vector Learning, B. Schölkopf and C. Burges and A. Smola (ed.), MIT-Press, 1999
[10] H. Lohninger*: Teach/Me Data Analysis*, Springer-Verlag, Berlin-New York-Tokyo, 1999
[11] L. Rutkowski "Adaptive Probabilistic Neural Networks for Pattern Classification in Time-Varying Environment", *IEEE Trans. on Neural Networks*, vol. 15pp. 811-827, July 2004
[12] The Mathworks: *Neural Networks Toolbox,* The Math Works Inc. 2000
[13] T. Lobos "Fast estimation of symmetrical components in real time", *IEE Proceeding*-C, Vol. 139, No 1, pp. 27-30, 1992
[14] T. Lobos, J. Rezmer, H-J. Koglin, "*Analysis of Power System Transients Using Wavelets and Prony Method", IEE Porto Power Tech Conference*, 10-13 September 2001, Porto, EMT-103
[15] S.G. Sanchez, N.G. Prelcic, S.J.G. Galan, (1996, Apr) *Uvi Wave-Wavelet Toolbox for Matlab* (ver 3.0), University of Vigo, Available: http://www.tsc.uvigo.es/~wavelets/uvi_wave.html